



A newly designed Cu/Super-P composite for the improvement of low-temperature performances of graphite anodes for lithium-ion batteries

M. Marinaro ^{a,*}, M. Mancini ^a, F. Nobili ^a, R. Tossici ^a, L. Damen ^b, R. Marassi ^a

^a Scuola di Scienze e Tecnologie, Sezione Chimica, Università di Camerino, Via S. Agostino 1, I-62032 Camerino (MC), Italy

^b Dipartimento di Scienza dei Metalli, Elettrochimica e Tecniche Chimiche, Università di Bologna, Via San Donato 15, I-40127 Bologna, Italy

HIGHLIGHTS

- Super-P supported Cu particles are synthesized via a microwave assisted procedure.
- The Cu/Super-P composite is used as conductive phase in graphite anodes.
- Cu-modified anodes show excellent electrochemical behavior at low temperatures.

ARTICLE INFO

Article history:

Received 6 April 2012

Received in revised form

30 July 2012

Accepted 22 August 2012

Available online 30 August 2012

Keywords:

Microwave-assisted synthesis

Carbon-supported copper nanoparticles

Conductive agent

Oxidized graphite

Low temperature electrochemical behavior

ABSTRACT

Copper nanoparticles supported on Super-P carbon (Cu/Super-P) are prepared by a one-pot microwave assisted procedure and used as conductive additive in graphite anodes for lithium-ion batteries. Anodes prepared with the Cu/Super-P additive show excellent cycling stability at temperatures as low as -30°C with reversible capacities of the order of 180 mAh g^{-1} . Four-points probe DC resistance measurements of layers prepared with Cu/Super-P demonstrate that the electronic resistance decreases of about half with respect to layers prepared with pristine Super-P. Additionally, the ac-impedance of Cu-modified electrodes is much lower than that of electrodes containing Super-P only. This implies an active role of the copper nanoparticles in improving the intercalation capacity, especially at low temperature.

© 2012 Elsevier B.V. All rights reserved.

1. Introduction

Nowadays graphite represents the state-of-the-art anode material for lithium-ion batteries. Despite its favorable properties such as a specific capacity of 372 mAh g^{-1} and the flat and low working potential close to that of pure lithium [1], the use of graphite is subjected to some limitations. For instance, the low rate capability and the poor electrochemical behavior at low temperature are well documented in the literature [2–5]. The reduced ability of graphite to intercalate lithium at low temperatures has been attributed to several factors: (i) high charge-transfer resistance at the electrolyte/electrode interface, (ii) low conductivity of the solid electrolyte interphase (SEI) and/or of the bulk electrode

(iii) reduced solid state lithium diffusivity within graphene sheets at temperature below -20°C . Several strategies have been pursued to overcome these limitations [6–12]. In this context, the use of metal particles dispersed in the electrodes bulk is effective in enhancing the low-temperature lithium intercalation ability of graphite electrodes [13,14]. Among different metals, copper has been demonstrated to be one the most effective “additive” for the design of graphite electrodes addressed to low-temperature applications. Different approaches have been reported for adding low amounts of metal particle to graphite anodes [13–15]. However, the mechanism determining the better low temperature behavior is not yet completely understood.

Super-P carbon is commonly used as additive to improve the electronic conductivity of electrodes for lithium-ion batteries. In this paper we describe an attempt to combine the positive effects of Super-P and metal nanoparticles by preparing copper nanoparticles supported on Super-P (Cu/Super-P) to be used in the electrodes formulation. The synthesis is performed via a microwave-assisted

* Corresponding author. Present address: Zentrum für Sonnenenergie- und Wasserstoff-Forschung Baden-Württemberg, Helmholtzstr. 8, D-89081 Ulm, Germany. Tel.: +49 (0)731 9530 406; fax: +49 (0)731 9530 666.

E-mail address: mario.marinaro@zsw-bw.de (M. Marinaro).

polyol procedure. This synthesis route, widely used for catalysts for fuel-cell applications [16,17], has never been used to the best of our knowledge for preparing conductive additives for lithium-ion battery electrodes. The microwave-assisted procedure presents several advantages with respect to other proposed strategies for introducing metals in the electrode bulk [13,14]. For example, metal nanoparticles mechanically mixed with conductive carbons tend to oxidize and form aggregates. Besides the relatively cheapness and easiness, the one-step synthesis presented in this paper provides a simple way to obtain stable and well dispersed copper nanoparticles. The use of the Cu/Super-P composite in the electrodes formulation leads to remarkably higher reversible capacities in the temperature range 20 to -30 °C than those of anodes prepared with pristine Super-P or using mechanically mixed Super-P copper nanoparticles. In the attempt to explain the reasons of the improvement of the low temperature intercalation capacity, electrochemical impedance spectroscopy and DC-resistivity measurements of the Cu-Super-P/graphite and Super-P/graphite electrodes are presented.

2. Experimental

2.1. Synthesis of Cu/Super-P composite

Super-P supported copper nanoparticles were synthesized following a microwave-assisted modified polyol procedure. In a typical synthesis, 25 ml of a $\text{CuSO}_4 \cdot 5\text{H}_2\text{O}$ (Aldrich; >99%) 0.01 M solution in ethylene glycol (EG) was mixed with 0.185 g of Super-P (Timcal) in a flask equipped with a water cooled condenser. The suspension was stirred for 30 min and then 25 ml of a solution of $\text{NaH}_2\text{PO}_2 \cdot \text{H}_2\text{O}$ (Aldrich) 0.02 M in EG were slowly added under vigorous agitation. After additional stirring the reaction mixture was irradiated for 5 min under medium power (540 W) using a modified domestic microwave oven. Agitation was continued during irradiation and the reactant mixture reached a temperature of about 200 °C. After cooling, the suspension was centrifuged and the final solid product, Cu/Super-P 8:92 weight ratio, was washed with acetone several times before being dried first at 50 °C in air and then at 200 °C under vacuum over-night.

2.2. Structural and morphological characterization of Cu/Super-P composite

The Cu/Super-P composite has been characterized by Scanning Electron Microscopy (SEM Cambridge Stereoscan mod. 369), Energy Dispersive X-ray spectroscopy (EDX) and X-ray spectroscopy using a Philips diffractometer equipped with a Cu K_α source ($\lambda = 0.154$ nm) and a $\theta/2\theta$ Brag-Brentano geometry. The average particle size has been calculated from XRD patterns according to the Scherrer's equation.

2.3. Electrodes preparation and electrochemical measurements

Electrodes were prepared according to a well-established procedure [13,14]. Timrex KS-15 (Timcal) graphite, partially oxidized in air at 750 °C for 45 min was used as active component. The oxidation degree was roughly estimated by the weight loss (30%). The oxygen content, determined by elemental analysis was of the order of 11%. Graphite anodes were prepared by "doctor blade" technique using slurry with the following composition: oxidized graphite KS-15:Super-P:PVdF in NMP with mass ratio 77.5:12.5:10. The slurry, after homogenization by magnetic stirring, was coated onto a copper foil (wet thickness of 250) and dried over-night at 60 °C. The same procedure was used to prepare copper-modified electrodes where the synthesized Cu/Super-P composite

replaced pristine Super-P leading to a final metal content of about 1 wt.%. The loading of all the obtained electrodes was about 2.5 mg cm⁻² based on the active material content.

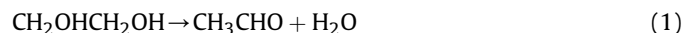
Electrochemical measurements have been carried out using T-shaped 3-electrode cells with stainless steel current collectors. Pure lithium foil by Foote Mineral Co. was used as counter and reference electrodes. Dried polypropylene film (Celgard 2400) and 1 M LiPF₆ in EC:DMC:DEC 1:1:1 (LP71 by Merck, battery grade) were used as separator and electrolyte, respectively. All cells were assembled in a glove-box filled with Ar. The low-temperature experiments have been carried out over the temperature range 20 to -30 °C using a freezer capable to control the temperature within ± 0.5 °C. Charge/discharge cycles were carried out within the potential window 0.01–1.5 V using a VMP 2/Z (Bio-Logic, France). Electrochemical impedance spectroscopy (EIS) has been performed using 3-electrode coin cells (EL-CELL, Germany) with metal Li as counter and reference electrodes and glass fiber (EL-CELL, Germany) as separator. The impedance spectra were collected by superimposing a sinusoidal potential oscillation of ± 5 mV, in the frequency range 100 kHz to 2 mHz, over a bias potential of 0.090 V. All the potentials are given vs. Li^+/Li .

DC-resistance has been measured at room temperature using a four-point probe technique. The samples were prepared starting from two different slurries (in NMP) having the following compositions: (i) oxidized KS-15:Super-P:PVdF 77.5:12.5:10 and (ii) oxidized KS-15:Cu/Super-P:PVdF 77.5:12.5:10. Each slurry has been coated (wet thickness 150 μm) onto Mylar foil by doctor blade technique and subsequently dried (dry thickness 65 μm).

3. Results and discussion

3.1. Synthesis and characterization of Cu/Super-P

The Cu/Super-P composite (weight ratio 8:92) has been synthesized following a microwave-assisted modified polyol procedure. In a generic polyol reaction, ethylene glycol (EG) can directly reduce metal ions once irradiated by microwaves. The entire process can be summarized by the following two reactions:



Moreover the use of sodium hypophosphite increases the reduction rate as from the following reaction:



In order to prevent particles aggregation and growth a surfactant agent/stabilizer such as polyvinylpyrrolidone (PVP) is often used in microwave-assisted polyol procedures [18–20]. In our approach Super-P carbon is used instead of PVP in order to overcome this issue. Indeed, the interaction between carbon and microwaves creates hot spots on the carbon surface that can facilitate the reduction by forming sites for heterogeneous nucleation of copper nanoparticles on the carbon surface [20]. The uniform formation of hot spots accelerates the reduction of metal precursors leading to uniform nanoclusters with small sizes. This type of procedure is rather common for the preparation of catalysts for fuel cells, such as carbon supported Pt [16] or Pt/Ru [17] nanoparticles.

Fig. 1(a) shows the SEM images of the Cu/Super-P composite. The corresponding backscattered electrons micrographs, reported in Fig. 1(b), clearly shows white spots that reveal the presence of copper particles well dispersed within the carbon matrix. Even for the largest agglomerates, the particles size never exceeds 1 μm . EDX

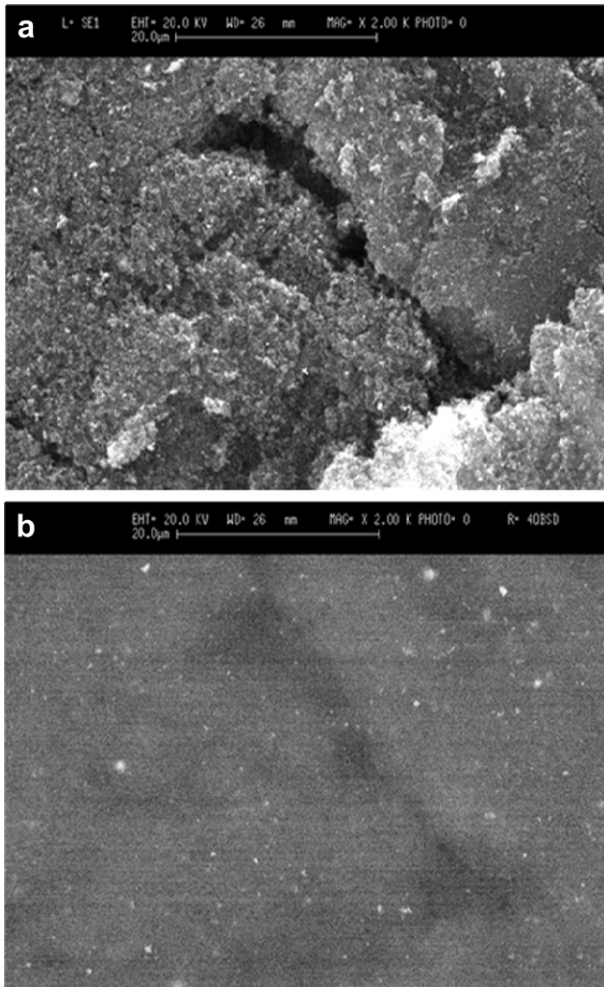


Fig. 1. SEM images of the synthesized Cu/Super-P composite. (a) Secondary electrons micrograph and (b) backscattered electrons micrograph.

spectroscopy (Fig. 2) confirms the presence of copper in the carbon matrix, as revealed by the $K\alpha_2$ (8.03 keV) and $K\beta_{1,3}$ (8.90 keV) emission lines.

Fig. 3 shows the X-ray diffractogram of the sample obtained in the 20–55° 2θ range. The broad peak centered at about 25° can be

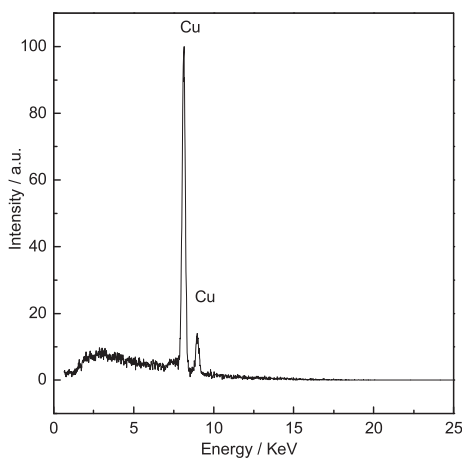


Fig. 2. EDX spectrum of the Cu/Super-P composite.

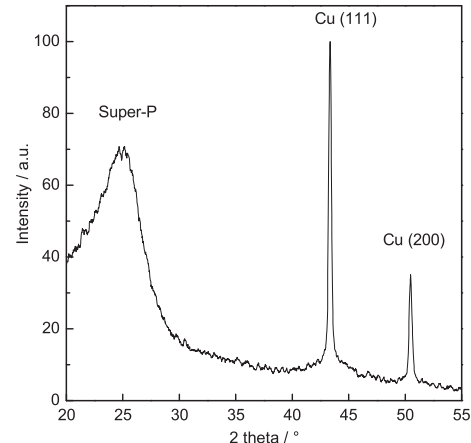


Fig. 3. XRD pattern of the Super-P supported Cu nanoparticles.

assigned to the amorphous Super-P carbon. The two peaks at 43.3° and 50.4° can be indexed as Cu (111) and Cu (200) reflections. The average size of the copper particles as estimated using the Scherrer's equation is of the order of 40 nm.

3.2. Electrochemical characterization

The electrochemical performances of graphite electrodes prepared with Cu/Super-P composite as conductive agent have been investigated by galvanostatic cycles at different temperatures between 20 and –30 °C. For sake of comparison, graphite electrodes prepared with pristine Super-P have also been characterized. Before running the experiments at low-temperature all the electrodes were cycled three times at room temperature and C/3 rate in order to form a stable SEI over the electrode surface. The irreversible capacity loss (ICL) at the first cycle is 180 mAh g^{–1} and 150 mAh g^{–1} for electrodes containing Cu/Super-P and pristine Super-P, respectively. This finding is in good agreement with previous results [13,14] and suggests a different path of the SEI formation for the two types of electrode.

Low-temperature tests have been performed by galvanostatic cycles at C/5 rate at 20, 10, 0, –10, –20 and –30 °C. At each temperature the cells were conditioned at OCV for at least 3 h and then continuously cycled for 5 times. Fig. 4(a) and (b) shows the galvanostatic profiles of the fifth lithium insertion, collected at different temperatures, for electrodes containing Cu/Super-P and pristine Super-P, respectively. Fig. 5 shows the evolutions of the average capacities as a function of the temperature for both kinds of electrodes. At room temperature, the intercalation capacities (computed on the basis of the graphite content) of both anodes are close to the theoretical value for graphite (372 mAh g^{–1}). At temperatures below 20 °C significant differences are observed. The electrode containing the Cu/Super-P composite has a specific capacity close to 340 mAh g^{–1} at –10 °C. At –20 °C and –30 °C the corresponding values are 280 and 178 mAh g^{–1}, corresponding to intercalation degrees (x) of 0.75 and 0.48 in Li_xC_6 . It is worth to note that at –30 °C, the electrode containing Cu/Super-P is able to retain almost 50% of the capacity achieved at 20 °C. On the other hand, the electrode containing pristine Super-P loses intercalation capacity rather rapidly starting at –10 °C to reach a value of about 40 mAh g^{–1} at –30 °C.

The differential capacity profiles dQ/dE^{-1} vs. E , computed from the galvanostatic curves, can be used to gain additional information on lithium loading/unloading processes. Fig. 6(a) and (b) shows curves for the Cu-modified and unmodified electrodes at

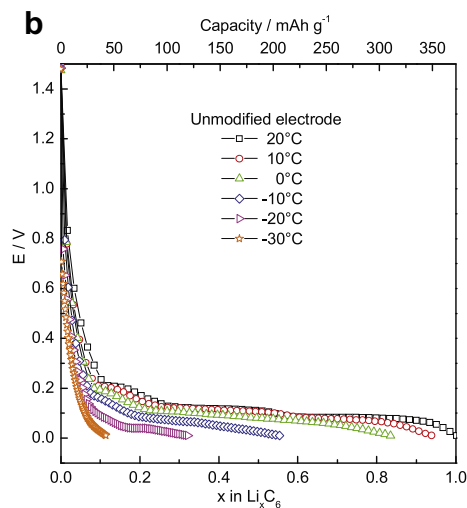
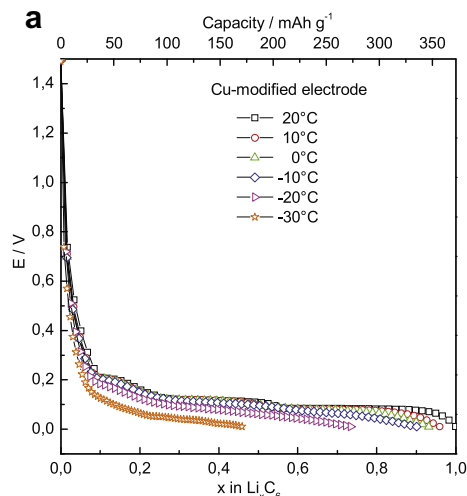


Fig. 4. Intercalation profiles of the Cu-modified electrode (a) and unmodified electrode (b).

20 °C and -20 °C, respectively. At 20 °C, the two profiles show similar shape and well resolved peaks, corresponding to the lithium staging processes into graphite. By lowering the temperature, kinetics of the involved processes are slowed down. As a result, the electrodes suffer from higher polarization that causes a shift of the peaks toward more negative/positive potentials during reduction/oxidation. The comparison of the differential profiles at -20 °C (Fig. 6(b)) clearly shows lower polarization of the electrode containing the Cu/Super-P additive. In the differential profiles of the Cu-modified electrode the peaks corresponding to the Li_xC stages are still distinguishable, whereas they are no longer visible in the plot of the unmodified one. The incomplete phase transition, due to high polarization at very low temperature, limits the intercalation capacity of the unmodified electrodes while the use of the Cu/Super-P improves the graphite lithium intercalation ability by decreasing the electrode polarization.

The effect of copper in reducing the polarization and increasing the low-temperature capacity of graphite electrodes has already been observed [13]. However, the low-temperature capacities obtained by the electrodes containing the new Cu/Super-P

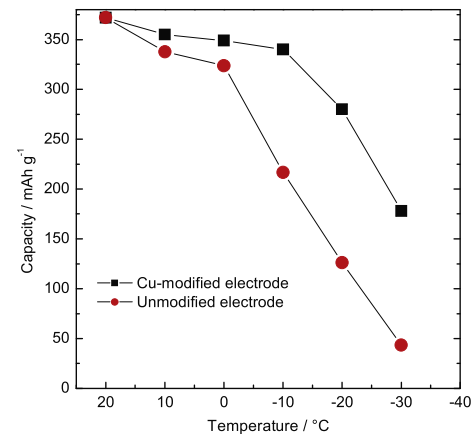


Fig. 5. Comparison between average values of the intercalation capacities (C/5 rate) for the Cu-modified (squares) and unmodified (circles) electrodes.

composite are the highest ever reported to the best of our knowledge. This improvement can be ascribed to the method used in the present work for introducing the metal in the electrode bulk. In fact, the one-pot synthesis of the Cu/Super-P allows obtaining copper particles smaller than those prepared by mixing Super-P with commercially available copper powder [13]. In addition, the in-situ formation of carbon supported copper

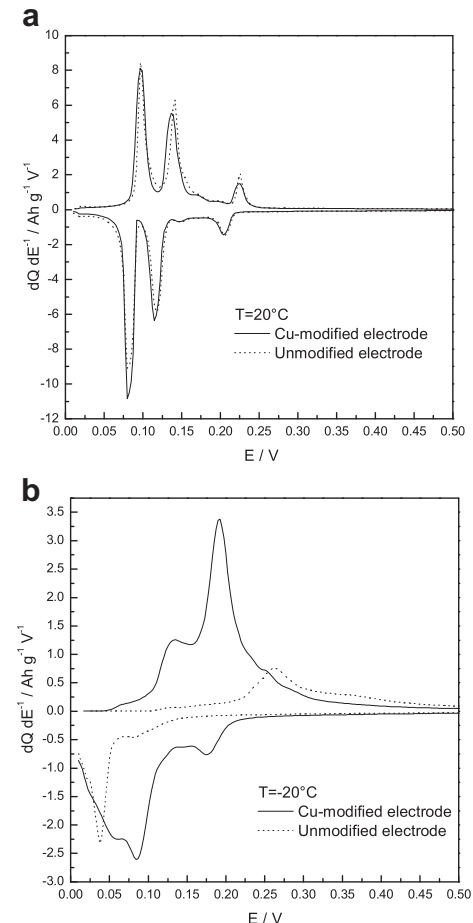


Fig. 6. Differential capacity profiles for Cu-modified and unmodified (dotted) electrodes at 20 °C (a) and -20 °C (b).

nanoparticles probably stabilizes the metal by preventing its oxidation and aggregation during air exposure and the electrodes fabrication steps. This effect is proven by the stability of the electrochemical behavior upon long-term cycling, as shown in Fig. 7 where the evolution of the reversible capacity at -30°C is reported. During the first 25 cycles the capacity increases from 120 to 175 mAh g^{-1} with successive cycling indicating that the electrode is slowly being “conditioned”. This behavior can be probably attributed to increased electrochemical access to active material as cycling proceeds. The capacity of the electrode remains constant afterward. The Coulombic efficiency is above 99% all over 100 cycles.

3.3. Electrochemical impedance spectroscopy

The role of metal nanoparticles dispersed in the electrode bulk in enhancing the low-temperature or high-rate electrochemical performances of graphite anodes has not yet been completely understood. Huang et al. [15] were the first who demonstrated an improvement of the electrochemical behavior of graphite anodes modified by the dispersion of copper or copper oxide particles in the electrode bulk. They hypothesized that the metal leads to a reduction of the energy needed by lithium ions to approach the graphite surface and to be available for charge-transfer. In particular, metal particles can play a catalytic effect toward the rate of lithium-ion desolvation process, occurring at the surface of the active material, thus decreasing the activation energy related to the charge-transfer that is the rate-limiting step of the lithium intercalation process [21–26]. In previous papers [13,14,27], the role of Cu and Sn metal dispersions in enhancing graphite intercalation performances was studied by galvanostatic cycling, cyclic voltammetry, and electrochemical impedance spectroscopy. Consistent experimental evidences were obtained demonstrating that the intercalation kinetics is strongly enhanced by metal dispersions and that the metal particles play an active role in enhancing the Li^+ ions desolvation rate at electrode/electrolyte interface. In this context, the low-temperature EIS response of the graphite anode containing the Cu/Super-P composite as conductive additive is here compared with that of the anode containing only Super-P carbon.

Fig. 8 shows the Nyquist plots of the two types of electrodes under investigation, acquired at $T = -20^{\circ}\text{C}$ and $E = 0.09\text{ V}$. Both electrodes show a behavior typical of graphite anodes, the main feature being the middle frequency semicircle related to charge-

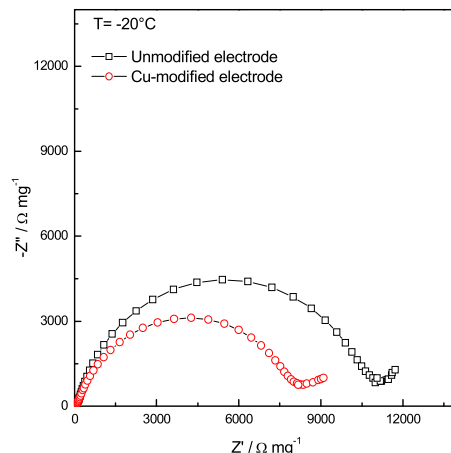


Fig. 8. Nyquist plots recorded at -20°C for electrodes Cu-modified (circles) and unmodified (squares) at a bias potential of 0.09 V .

transfer process. In addition, a high-frequency shoulder (hardly noticeable due to overlapping by the main semicircle) reveals the presence of a solid electrolyte interphase (SEI), while the low-frequency $\pi/4$ line describes Li^+ diffusion. Similar results, not reported for sake of brevity, have been obtained at other temperatures. As it may be seen the overall impedance of the Cu/Super-P modified electrode is lower than that of the unmodified electrode. The experimental dispersions have been fitted to the equivalent circuit extensively used for intercalation electrodes [14,27–29] and summarized, by using Boukamp's notation [30], as $R_{\text{el}}(R_{\text{sei}}C_{\text{sei}})(R_{\text{ct}}C_{\text{dl}})W$, where R_{el} , R_{sei} and R_{ct} represent the resistances respectively associated with electrolyte, passivation layer and charge-transfer process, C_{sei} and C_{dl} describe the capacitances of passivation layer and double layer, W is the Warburg impedance due to diffusion. During the fitting procedure, all C elements have been substituted with constant phase elements Q in order to take into account any deviations from ideal behavior, due to inhomogeneities and roughness in composition and morphology of electrodes and passivation layers [31]. The fitting procedure gave a χ^2 of the order of 10^{-4} . The computed R_{ct} values are 1.1×10^4 and $8 \times 10^3\text{ Ω mg}^{-1}$, corresponding to 1.4×10^4 and $1.0 \times 10^4\text{ Ω cm}^2$, for the electrodes containing pristine Super-P and Cu/Super-P respectively, confirming that the dispersion of copper nanoparticles within the composite electrode enhances the low temperature interfacial charge-transfer kinetics. The other effect that contributes to the enhancement of the low temperature electrochemical behavior is the decreased bulk resistance of the Cu-modified electrodes as demonstrated by the four-point resistance measurements. The relevant values at 20°C , listed in Table 1 show that the DC resistance of the Cu-modified electrodes is almost one half of the one of the unmodified electrodes. Less bulk resistance together with the decreased charge-transfer resistance translates into decreased electrode polarization as also demonstrated by the differential

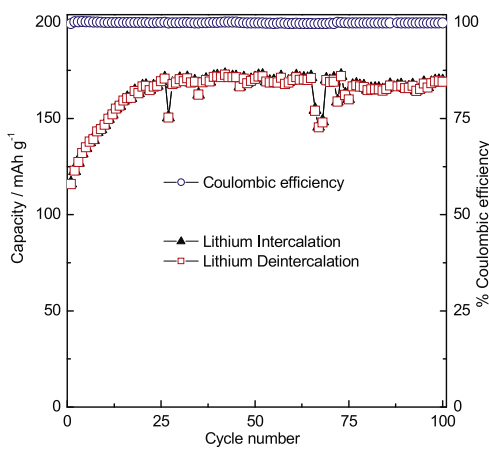


Fig. 7. Cycling stability and Coulombic efficiency of the Cu-modified electrode over 100 cycles at -30°C with a charging/discharging rate of C/5.

Table 1

Values of the electrical resistance (R in Ω) and resistivity (ρ in $\Omega \text{ cm}$) obtained from DC experiments.

	$R = K(V/i)$ [Ω]	$\rho = R_t$ [$\Omega \text{ cm}$]
KS-15ox + Cu/Super-P	18.97	0.1233
KS-15ox + Super-P	33.23	0.2160

capacity plots of Fig. 6. The final result is an improved lithium intercalation ability of the Cu-modified electrodes.

4. Conclusions

A new Cu/Super-P conductive additive for graphite anodes for lithium-ion batteries has been synthesized by a microwave-assisted polyol procedure. The structural and morphological characterizations show carbon supported copper particles well dispersed throughout the carbon matrix, with dimension of about 40 nm. The Cu-modified anodes show remarkable improved performances in terms of higher reversible capacity at low temperatures. In particular, the capacity obtained at the lowest temperature, i.e. -30°C , is about 180 mAh g^{-1} stable upon continuous cycling. This behavior roots in an enhancement of the interfacial charge-transfer kinetics and in lower DC-electrical resistance. The reported results give a more comprehensive description of the role of metal particles in improving the electrochemical behavior of graphite anodes. The enhancement of electrode performances in terms of capacity and polarization can thus be related to the contribution of concomitant effects of the copper particles: (i) a local effect due to the catalysis of lithium ions desolvation that accelerates the interfacial step of the charge-transfer process [14] and, (ii) an increasing of the overall electrode bulk conductivity that leads to a faster electron mobility especially at low temperatures. The low-temperature capacity and cycling stability of graphite anodes containing the Cu/Super-P additive, together with the relatively easy and cheap proposed synthesis route, make the use of the copper-based conductive agent extremely attractive for designing graphite electrode for low-temperature lithium ion batteries.

Acknowledgments

This work has been supported by the contract “Accordo di Programma MSE-ENEA sulla Ricerca di Sistema Elettrico 2011”.

References

- [1] M.B. Armand, in: D.W. Murphy, J. Broadhead, B.C. Steele (Eds.), *Material for Advanced Batteries*, Plenum Press, New York, 1980, p. 145.
- [2] C.K. Huang, J.S. Sakamoto, J. Wolfenstine, S. Surampudi, *J. Electrochem. Soc.* 147 (2000) 2893.
- [3] S.S. Zhang, K. Xu, T.R. Jow, *Electrochim. Acta* 48 (2002) 241.
- [4] H.P. Lin, D. Chua, M. Salomon, H.C. Shiao, M. Hendrickson, E. Plichta, S. Slane, *Electrochim. Solid-State Lett.* 4 (2001) A71.
- [5] G. Nagasubramanian, *J. Appl. Electrochem.* 31 (2001) 1999.
- [6] E. Peled, C. Menachem, D. Bar-Tov, A. Melman, *J. Electrochem. Soc.* 143 (1996) L4.
- [7] C. Menachem, E. Peled, L. Burstein, Y. Rosenberg, *J. Power Sources* 68 (1997) 277.
- [8] C. Menachem, Y. Wang, J. Flowers, E. Peled, S.G. Greenbaum, *J. Power Sources* 76 (1998) 180.
- [9] R.S. Rubino, E.S. Takeuchi, *J. Power Sources* 81–82 (1999) 373.
- [10] T. Prem Kumar, A.M. Stephan, P. Thayananth, V. Subramanian, S. Gopukumar, N.G. Renganathan, M. Raghavan, N. Muniandy, *J. Power Sources* 97–98 (2001) 118.
- [11] N.A. Asrian, G.N. Bondarenko, G.I. Yemelianova, L.Y. Garlenko, O.I. Adrov, R. Marassi, V.A. Nalimova, D.E. Skłowski, *Mol. Cryst. Liq. Cryst.* 340 (2000) 331.
- [12] X. Cao, J.H. Kim, S.M. Oh, *Electrochim. Acta* 47 (2002) 4085.
- [13] F. Nobili, S. Dsoke, T. Mecozzi, R. Marassi, *Electrochim. Acta* 51 (2005) 536.
- [14] M. Mancini, F. Nobili, S. Dsoke, F. D'Amico, R. Tossici, F. Croce, R. Marassi, *J. Power Sources* 190 (2009) 141.
- [15] H. Huang, E.M. Kelder, J. Schonman, *J. Power Sources* 97–98 (2001) 114.
- [16] Z. Liu, L.M. Gan, L. Hong, W. Chen, J.Y. Lee, *J. Power Sources* 139 (2005) 73.
- [17] Z.L. Liu, J.Y. Lee, W.X. Chen, M. Han, L.M. Gan, *Langmuir* 20 (2004) 181.
- [18] H. Zhu, C. Zhang, Y. Yin, *J. Cryst. Growth* 270 (2004) 722.
- [19] Y. Lee, J. Choi, K.J. Lee, N.E. Stott, D. Kim, *Nanotechnology* 19 (2008) 415604.
- [20] M. Tsuji, M. Hashimoto, Y. Nishizawa, M. Kubokawa, T. Tsuji, *Chem. Eur. J.* 11 (2005) 440.
- [21] P.G. Bruce, M.Y.J. Saidi, *Electroanal. Chem.* 322 (1992) 93.
- [22] K. Xu, Y. Lam, S.S. Zhang, T.R. Jow, T.B. Curtis, *J. Phys. Chem. C* 111 (2007) 7411.
- [23] K. Xu, *J. Electrochem. Soc.* 154 (2007) A162.
- [24] K. Xu, A. von Cresce, U. Lee, *Langmuir* 26 (2010) 11538.
- [25] T. Abe, H. Fukuda, Y. Iriyama, Z. Ogumi, *J. Electrochem. Soc.* 151 (2004) A1120.
- [26] T. Abe, F. Sagane, M. Ohtsuka, Y. Iriyama, Z. Ogumi, *J. Electrochem. Soc.* 152 (2005) A2151.
- [27] F. Nobili, M. Mancini, S. Dsoke, R. Tossici, R. Marassi, *J. Power Sources* 195 (2010) 7090.
- [28] F. Nobili, S. Dsoke, M. Mancini, R. Tossici, R. Marassi, *J. Power Sources* 180 (2008) 845.
- [29] F. Nobili, S. Dsoke, M. Mancini, R. Marassi, *Fuel Cells* 9 (2009) 264.
- [30] B.A. Boukamp, *Solid State Ionics* 20 (1986) 159.
- [31] E. Barsoukov, J. Ross Macdonald, *Impedance Spectroscopy: Theory, Experiments and Applications*, second ed., John Wiley & Sons, New York, 2005, p. 83.